Does high-resolution modelling improve the spatial analysis of föhn flow over the Larsen C ice shelf?

Turton,JV., Kirchgaessner, A., Ross, AN. and King, JC

Abstract

The ice shelves on the east coast of the Antarctic Peninsula (AP) have been disintegrating for over two decades. Surface melting induced by föhn winds has been proposed as a driver of this disintegration. Föhn winds are adiabatically warmed, dry winds, formed by the interaction of a mountain range with perpendicularly approaching winds, in this case of the AP mountains with the prevailing circumpolar westerlies. Assessing their impact is difficult due to sparse observations and relatively low-resolution operational forecasts. We have carried out high-resolution simulations using the Weather Research and Forecasting (WRF) model to provide more detailed simulations of the spatial distribution of the föhn air. The analysis presented here covers the period from May 10th to 22nd, 2011, and focuses on two föhn events during this period. Results show that a stable boundary layer can reduce the impact of föhn, as can the occurrence of cooler föhn jets.

Introduction

The Antarctic Peninsula (AP) mountain range stretches over approximately 1500km, from Drake Passage in the north, to Ellsworth Land in the south (Figure 1a). Its average elevation is 1500m, and approximately 80% of the area is permanently ice covered by ice sheets, glaciers or adjacent ice shelves. During the 20th century this was the fastest warming region on earth, however in the last 16 years, this warming has paused (Turner *et al.*, 2016).

The AP Mountains provide a barrier between the warm, maritime climate to the west, and the cold, continental climate to the east. Locations on the west coast are, on average, around 10°C warmer in annual mean temperature than those at the equivalent latitude and elevation on the east coast (Cook and Vaughan, 2010). Despite the cold eastern climate, several ice shelves have disintegrated, in particular Larsen A in 1995, shortly followed by Larsen B in 2002.

The Larsen ice shelf comprised of four ice shelves (Larsen A to D). Larsen C Ice Shelf is the focus of this study, and is the largest remaining ice shelf of the group (Figure 1b). Prior to 2013, it was largely believed that this ice shelf was stable for the foreseeable future. However, a rift has opened on the southeastern edge of the ice shelf and approximately 10% of ice volume may be lost in the near future (Jansen *et al.*, 2015). Calving of ice shelves is a natural process, but due to the location of the rift, the ice shelf may become unstable once the calving event has occurred.

One proposed theory for the destabilisation of ice shelves is the 'föhn hypothesis'. This has been studied over Larsen B by Cape *et al.* (2015) and the Larsen C ice shelf by Elvidge *et al.* (2015, 2016) amongst others. It theorises that föhn winds have increased in frequency due to a contraction and strengthening of the circumpolar vortex. The circumpolar vortex is a persistent low pressure system in the upper atmosphere, centred over the interior of the Antarctic continent that generates the predominant, westerly flow of air around the Antarctic. When westerly winds interact with the AP, warm and dry föhn winds can develop. They can induce and enhance surface melt on the ice shelf.

Due to the large spatial area, and remote location, observations of föhn winds using Automatic Weather Stations (AWS) are relatively sparse compared with, for example, European observational networks. We have used archived regional model output at 5km horizontal resolution to analyse föhn winds in conjunction with observations. However, the complex, local interactions with the boundary

layer can be misrepresented in the relatively coarse model output, leading to inaccuracies in quantifying the impact of föhn events. For global climate models, 5km horizontal resolution is very fine. However, for regional modelling of the AP region, finer resolution is required to accurately simulate the small topographical features, and to resolve boundary layer processes.

Using higher-resolution models (1.5km horizontal resolution) may provide additional information on the spatial distribution and the vertical structure of mesoscale features such as föhn events. However, running high-resolution models is computationally expensive and time consuming. A useful compromise is to simulate case studies of individual föhn events, such as those by Elvidge *et al* (2015, 2016). The case study presented here was conducted to assess the added benefits of using higher-resolution output, for modelling föhn events.

Föhn winds over Larsen C ice shelf

Föhn winds are predominantly generated by two processes; thermodynamic warming, and isentropic drawdown. Thermodynamic, or 'classical' föhn theory, is the textbook föhn development (Figure 2a).

Low level air masses with sufficient momentum can ascend the windward (western) side of the AP. The ascending air initially cools at the dry adiabatic lapse rate (10K km^{-1}) but, once condensation and precipitation occurs, it continues to ascend at the approximate saturated adiabatic lapse rate of 6.5K km^{-1}. Once the air mass overcomes the mountains, it descends down the lee slope and, having lost moisture on the upwind slope, warms at the dry adiabatic lapse rate of 10K km^{-1}. Consequently the air mass is adiabatically warmer, and drier, than air at the same altitude on the windward side of the mountain.

The second mechanism is isentropic drawdown (Figure 2b). Low level blocking of air on the windward side of the mountains prevents ascent of the air mass. During westerly winds, this blockage causes advection of potentially warmer and drier air from aloft.

Föhn onset is characterised by a decrease in relative humidity and an increase in air temperature. Sometimes, an increase in wind speed also occurs. Föhn events are frequent and spatially extensive over Larsen C. They can reach over 250km in the north-south direction, and up to 130km in the west-east direction in observations and in a 5km horizontal resolution model (Turton, 2017).

Data and Methods

Observational data from two AWS sites were used to validate the model output. AWS1 is located at approximately 400m a.s.l on Cole Peninsula, an outcrop at the foot of the AP. AWS2 is located at a distance of ~130km from the AP, on the flat, homogeneous ice shelf (Figure 1b). Air temperature, relative humidity, wind direction and wind speed observations from both AWSs have been averaged into six-hourly time points centred on 00, 06, 12 and 18UTC from 10th May, 00UTC to 22nd of May, 00UTC.

For this study, model data from two configurations of the Polar Weather Research and Forecasting (WRF) model were used. Polar WRF is a modified version of the WRF model in which parameterisations of surface, boundary layer and cloud processes have been optimised for more accurate simulation of the polar atmosphere (Hines and Bromwich, 2008).

The first configuration of Polar WRF was used in the Antarctic Mesoscale Prediction System (AMPS), run by the National Center for Atmospheric Research, USA. AMPS was originally developed for operational support for the US Antarctic Program (Powers *et al.*, 2012), and has archived 5km horizontal resolution forecasts for the AP for the period of interest. For more information on the set

up of AMPS and WRF see Powers *et al.*, (2012). Archived AMPS data were used as the coarser-resolution output, and are referred to as '5km' in this article.

The second configuration of Polar WRF has a horizontal resolution of 1.5km and an enhanced vertical resolution, increasing the number of levels from 44 in the 5km run, to 70 in the 1.5km run. This was run from the 10th to 22nd May 2011 (the case study period) to simulate two föhn events. Output from this simulation is referred to as '1.5km'. Data have been extracted at 00, 06, 12 and 18UTC to compare with observations.

The föhn events were identified prior to this study using two algorithms for detection. Briefly, the six-hour averaged data must meet a number of requirements in both the observations and model output. At AWS1 (AWS2), the observed relative humidity must be below 52% (73%), or 59% (79%) if accompanied by a temperature rise of 3°C (Turton, 2017). The different thresholds allow for the föhn air characteristics to weaken as it propagates across the ice shelf. For both locations a decrease in relative humidity of at least 15% over 12 hours also indicated föhn air. These thresholds were chosen after climatological analysis of the data revealed relatively low frequency but extremely dry and warm conditions. To identify a föhn period from the 5km model data, the method developed for detecting föhn winds over South Georgia by Bannister and King (2015), was adapted for use over the AP. The potential temperature upwind of the AP (in undisturbed flow) and just above the height of the AP (~2000m) was tracked eastwards, over the AP. On the lee side, the minimum altitude of the same potential temperature was located. If the change in height of the potential temperature, from its upwind elevation to the lee side elevation, was greater than 500m then a föhn event was identified.

Results

Observed characteristics at AWS1

Two föhn events were identified at AWS1. The first föhn event (föhn #1) spanned 84 hours from 18UTC 11th to 06UTC 15th May 2011 (Figure 3). This event was characterised by a rapid decrease in relative humidity from 84% prior to the event to 22%, 30 hours into the event (Figure 3a). The increase in air temperature was also fairly rapid, rising from -25.5°C prior to the event to 5.1°C 96 hours later (Figure 3b). The wind speed remained low with an average of 3.7ms^{-1}. The end of this föhn event was less well defined due to a gradual increase in relative humidity, and no decrease in temperature. The wind direction turned from northwesterly to southeasterly, which indicated cessation of the föhn.

Föhn #2 was shorter (42 hours), spanning from 00UTC 16th to 18UTC 17th May 2011. The relative humidity decreased in steps down to a minimum value of 37% (Figure 3a). The average temperature was warmer than during the first föhn event (4.7°C) (Figure 3b). The wind direction was also more variable, although the wind speed was higher (6.0ms^{-1}). The end of the föhn event was marked by a 15.5°C drop in temperature, and a steep (29%) rise in relative humidity.

Observed characteristics at AWS2

Two föhn events were identified at AWS2, but they were shorter than at AWS1, as the föhn air had to travel across the ice shelf, and interact with a stable boundary layer before being observed at AWS2. Föhn #1 persisted for 12 hours, from 00UTC to 12UTC 15th May 2011. Its onset was characterised by a very sharp drop in relative humidity of 18% in six hours (Figure 3c). The air temperature rise was more gradual, increasing from -28.3°C (at 00UTC 14th May) to 0.5°C (at 06UTC 15th May) (Figure 3d).

The wind speed peaked at 11.5ms^{-1}. The end of the föhn event was marked by an increase in relative humidity and the wind direction became northeasterly.

Föhn #2 was 18 hours long from 00UTC to 18UTC 16th May 2011. The onset was characterised by a large decrease in relative humidity to a minimum of 67% (Figure 3c). The air temperature increased by 2.7°C at föhn onset (Figure 3d). The wind direction returned to northwesterly and wind speed increased (8.9ms^{-1}) for a short period. A gradual decrease in air temperature, and a stepped increase in relative humidity marked the end of the event.

Simulation of near-surface characteristics

The föhn events were captured by both the 5km and 1.5km resolution model data, but with varying degrees of success. The simulations of the near-surface characteristics throughout the case study were more accurate at AWS1, with smaller biases than at AWS2 (Table 1).

At AWS1 the initial decrease in relative humidity which characterised the onset of föhn #1 was simulated relatively well by both runs (Figure 3a), however the very low relative humidity values were not captured. The relative humidity during föhn #2 was better modelled than föhn #1. Overall, the 1.5km run had smaller humidity biases than the 5km run at AWS1.

The air temperature was represented very well by both models at AWS1. The peak in temperature on the 13th May was not captured by either run (Figure 3b). The 1.5km run had slightly smaller mean biases than the 5km run for air temperature.

During non-föhn conditions at AWS2, the 5km run simulated the relative humidity with greater accuracy. The 1.5km run underestimated the relative humidity, which lead to larger mean biases and poor correlation with the observations (Table 1). However, during föhn conditions, the 1.5km run performed better. The timing of the relative humidity decrease at föhn #1 onset was simulated too early by the 5km run.

At AWS2 the air temperature was overestimated by both model runs prior to the föhn onset, but increased in accuracy during the föhn events. The stepped decrease in temperature after föhn #2 had ended was well simulated by the 1.5km run.

At AWS1 the wind speed was largely overestimated by both resolution models, however the accuracy was improved at AWS2. Both resolution runs had difficulty simulating the wind direction (not shown).

Spatial Distribution of Föhn Events

The limited observations available provide an incomplete picture of the spatial structure of föhn events. A regional model can provide additional spatial details and high-resolution models can reveal features such as gap flows, localised enhancements and other small-scale phenomena.

The 1.5km run has revealed that the spatial extent of the two föhn events was different. During föhn #1, propagation of föhn air across the ice shelf was slow. The increase in temperature was observed at the foot of the mountains for two days, but the near-surface temperature over most of the ice shelf remained below -10°C for the majority of the event. This was due to the presence of a cold, stable boundary layer over the ice shelf. The föhn winds had to erode this cold air as they propagated eastwards. By the end of föhn #1, the air temperature across the ice shelf was 0-2°C, with some areas close to the foot of the AP as warm as 4°C, allowing for widespread surface melting to occur for some (but not the entire duration) of the event.

As föhn #1 had already removed the cold air pool over the ice shelf, the warming signal during föhn #2 was widespread from the onset onwards. However, the impact of the warm winds was reduced by the presence of bands of cool, moist air in the '1.5km' run (Figure 4b). These 'föhn jets', as described by Elvidge *et al.* (2015), are a type of gap flow, which introduce cool and moist air into the surrounding föhn air. As the jet-air flows through gaps and passes in the mountain range rather than ascending and descending the full height of the AP, it experiences less cooling on the windward side, and less warming on the lee side of the AP (Elvidge *et al.*, 2015).

These jets were not static over the ice shelf. The cessation of föhn #2 at AWS2 was likely due to one föhn jet moving over the location, whereas at AWS1, the föhn event continued for a further 30 hours. The interaction between the föhn air and the föhn jets has implications for the surface energy budget and the spatial distribution of föhn-induced melting and sublimation when temperatures are above freezing.

Three elongated föhn jets were clearly visible in the temperature output from the '1.5km' run, orientated in a northwest to southeast direction. However, in the '5km' only small patches of cool air were simulated (Figure 4a), which did not resemble the thin, elongated shape of the jets. The jets were also not visible in the relative humidity output from the 5km run.

The end of föhn #2 at AWS1 was characterised by the displacement of the warm air by an incoming cooler air mass. At 00UTC on the 18th May, a cold, southerly flow pushed colder air over the ice shelf, and removed the föhn air from the foot of the AP Mountains. The '1.5km' run accurately modelled the timing of the cold air advancement. In the '5km' data, this cold air mass arrived earlier, and was spread north over the ice shelf faster, bringing föhn conditions to an earlier end.

Vertical Structure of Föhn Flow

The isentropic drawdown was present in both simulations. The vertical structure of the föhn winds was represented somewhat more clearly by the '1.5km' run (Figure 5). This simulated two dips in potential temperature, are likely due to the presence of a hydraulic jump, where the faster flowing air over the AP meets the relatively stationary air on the lee side. The smaller-scale topography likely controls the location of the hydraulic jump. The hydraulic jump was not represented in the '5km' run. Instead, a broader area warm-air advection was present (Figure 5).

The asymmetry in low-level air temperature between the windward and leeward side of the mountain during föhn events was more clearly simulated by the '1.5km' run. In the '5km' run, the cold air pool was still present on the ice shelf, however in the '1.5km' run the föhn air had penetrated to the surface. The '1.5km' run therefore resolved the erosion of the cold pool by the föhn winds better than in the '5km' run.

 The improved representation of the topography in the high-resolution model (Figure 5b) likely contributed to more clearly-defined isentropic drawdown and the simulation of the föhn jets.

Discussion

The purpose of this study was to evaluate the representation of föhn winds in coarser (5km) and higher (1.5km) resolution modelling, and assess the additional spatial information gained from using a high-resolution model. Running high-resolution models is both costly and time consuming, which limits the current study to a 12-day case study. However, for mesoscale features such as föhn events, especially in the observationally-sparse Antarctic, high-resolution modelling is crucial for understanding the spatial distribution, vertical structure and near-surface characteristics of the events.

The biggest advantage of using a higher-resolution model is the representation of small-scale features. Föhn jets, which stretched across the ice shelf, and intersected the warmer, drier föhn air throughout the second föhn event, were simulated only by the 1.5km run. These features were first identified in the Met Office Unified Model and in aircraft observations by Elvidge *et al.* (2015). The 5km resolution model failed to capture the shape and extent of the föhn jets as clearly as the '1.5km' run.

The föhn jets may be responsible for the poor correlation and large mean biases at AWS2. With AWS1 being situated at the foot of the AP, almost all descending föhn air will be captured by both the observations and the model. The important role föhn jets and the stable surface layer play at AWS2, complicates matters here. If the model misrepresents the location, spatial extent, or timing of the föhn jet, then observations and model are likely to disagree significantly. Similarly, if the model does not accurately resolve the topography, including the gaps that allow the jets to form, this will cause additional bias between the observations and simulations. The relative humidity values from observations and AMPS were calculated with respect to (w.r.t) ice when temperatures were below freezing, however the WRF case study output relative humidity w.r.t a mixed phase. This may cause a small amount of difference in the relative humidity values, however this isn't the case of the large mean bias at AWS2.

Increasing the vertical resolution provided more details about the structure of the föhn air. This may be crucial for assessing the impact of föhn winds on surface melt and sublimation. During much of föhn #1, a stable surface layer shielded the ice shelf from the warm, föhn air and reduced the duration of the warming. However, as the second föhn event arrived soon after the removal of the cold pool by föhn #1, near-surface warming from föhn #2 was extensive, and may have caused widespread surface melting. This was not simulated to the same extent by the '5km' run, which had an accordingly lower vertical and horizontal resolution.

Conclusion

High-resolution modelling has provided additional information on the interaction of föhn air with cold, stable surface layers over the Larsen C ice shelf, and the ability of föhn air to penetrate it. The propagation of the warm and dry air across the ice shelf was clearly simulated in the high-resolution run. Furthermore, föhn jets, which are the likely cause for the (early) cessation of föhn #2 at AWS2, were simulated by the 1.5km but not by the 5km model.

High-resolution models can more accurately assess the potential impact of föhn air on the surface energy balance, surface melting and sublimation of the Larsen C ice shelf, due to the more accurate representation of the atmospheric boundary layer and mesoscale features. However, until the available computing power increases, the use of such high-resolution models is limited to case studies, and lower-resolution models will have to be used for climatological studies. Comparing how high- and low-resolution models respectively simulate föhn winds, helps us to understand the strengths and weaknesses of the latter, thus enables us to understand the limitations of climatological studies carried out with lower-resolution models.

References

Bannister D, and King JC 2015. Föhn winds on South Georgia and their impact on regional climate. *Weather.* **70**(11): 324-329.

Cape MR, Vernet M, Skvarca P *et al* 2015. Foehn winds link climate-driven warming to ice shelf evolution in Antarctica. *Journal of Geophysical Research: Atmospheres.* **120**(21): 11037-11057.

Cook AJ, Vaughan DG 2010. Overview of areal changes of the ice shelves on the Antarctic Peninsula over the part 50 years. *The Cryosphere.* **4**: 77-98.

Elvidge AD, Renfrew, IA, King JC *et al* 2015. Foehn jets over the Larsen C ice shelf, Antarctica. *Quarterly Journal of the Royal Meteorological Society.* **141**: 698-713.

Elvidge AD, Renfrew IA, King JC *et al* 2016. Foehn warming distributions in nonlinear and linear flow regimes: a focus on the Antarctic Peninsula. *Quarterly Journal of the Royal Meteorological Society.* **142**(695): 618-631.

Hines KM, and Bromwich DH 2008. Development and testing of Polar WRF. Part 1. Greenland Ice Sheet Meteorology. *Monthly Weather Review.* **136**: 1971-1989.

Jansen D, Luckman AJ, Bevan S *et al* 2015. Brief communication: Newly developing rift in Larsen C ice shelf presents significant risk to stability. *The Cryosphere.* **9**(3): 1223-1227.

Powers JG, Manning KW, Bromwich DH *et al* 2012, A Decade of Antarctic Science Support Through Amps, *Bull. Amer. Meteor. Soc.*, **93**(11), 1699-1712, doi: 10.1175/bams-d-11-00186.1.

Turner J, Lu H, White I *et al* 2016. Absence of 21st century warming on Antarctic Peninsula consistent with natural variability. *Nature.* **535**: 411-415.

Turton, JV, Kirchgaessner, A., Ross, A *et al* 2017. *The spatial and temporal distribution of föhn winds on the Larsen C ice shelf, Antarctica.* PhD Thesis. University of Leeds.

Figure Captions:

Figure 1: a) Map of the Antarctic Peninsula region and bordering seas. Red markers 1 and 2 refer to AWS1 and AWS2 locations respectively. The Larsen C ice shelf is highlighted by the black box. b) Map of the Larsen C ice shelf, Antarctic Peninsula and Adelaide Island. Figures courtesy of MAGIC department at the British Antarctic Survey.

Figure 2: The thermodynamic (a) and isentropic drawdown (b) mechanisms responsible for föhn development over idealised topography.

Figure 3: a) The relative humidity and b) air temperature at AWS1 from the 10th to 22nd May 2011. c) The relative humidity and d) air temperature at AWS2 for the same period. The observations from the AWS are shown by black crosses. The '5km' output is shown as green dots, and that from the '1.5km' run as orange stars. The grey boxes indicate the periods when two föhn events occurred. Föhn #1 and föhn #2 are abbreviated to #1 and #2 for the AWS2 plots.

Figure 4: a) The 2m air temperature and 10m wind speed and direction simulated by the '5km' run and b) by the '1.5km' run. Output from both model runs is from 06UTC on the 16th May 2011, six-hours after the start of the second föhn event at AWS1 and AWS2 (green markers).

Figure 5: Cross section along 67°S of the Antarctic Peninsula of the simulated potential temperature (K) during föhn #2 from the '5km' run (a) and the '1.5km' run (b).

Table 1: The mean values, mean biases and correlation coefficient for air temperature, relative humidity and wind speed for the observations and both model runs from 10th-22nd May 2011. Green highlighted boxes are where the 1.5km resolution run was more accurate or the same as the 5km run. 'Obs' is the abbreviated version of observations.
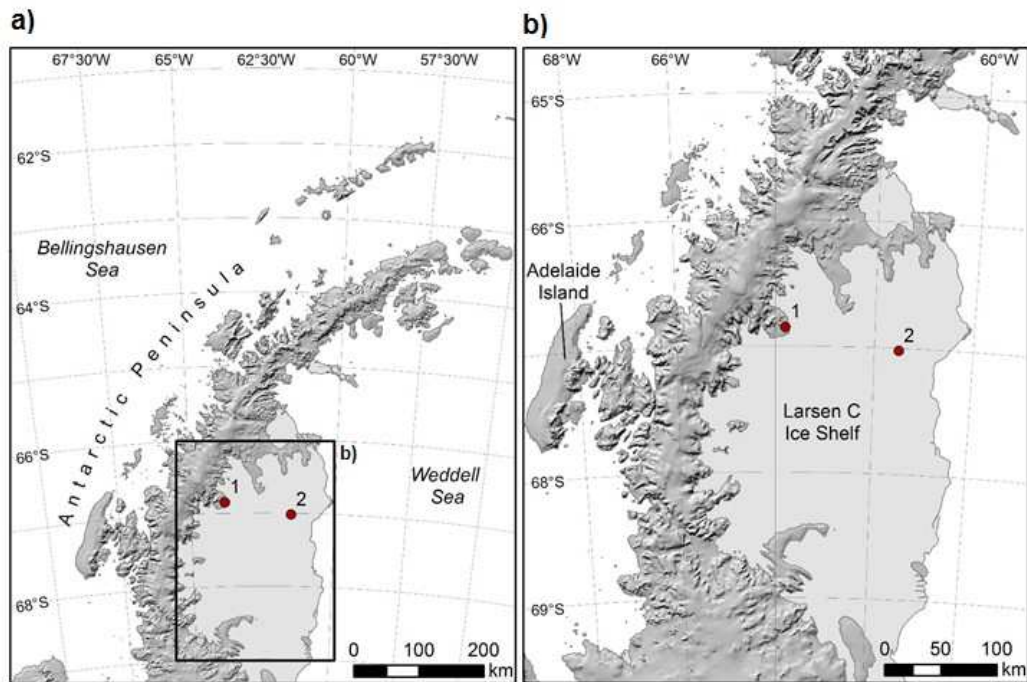
Figure 1: a) Map of the Antarctic Peninsula region and bordering seas. Box marked b) is the Larsen C ice shelf region corresponding to figure b. Markers 1 and 2 refer to the AWS1 and AWS2 locations respectively. Figures courtesy of MAGIC department at the British Antarctic Survey.
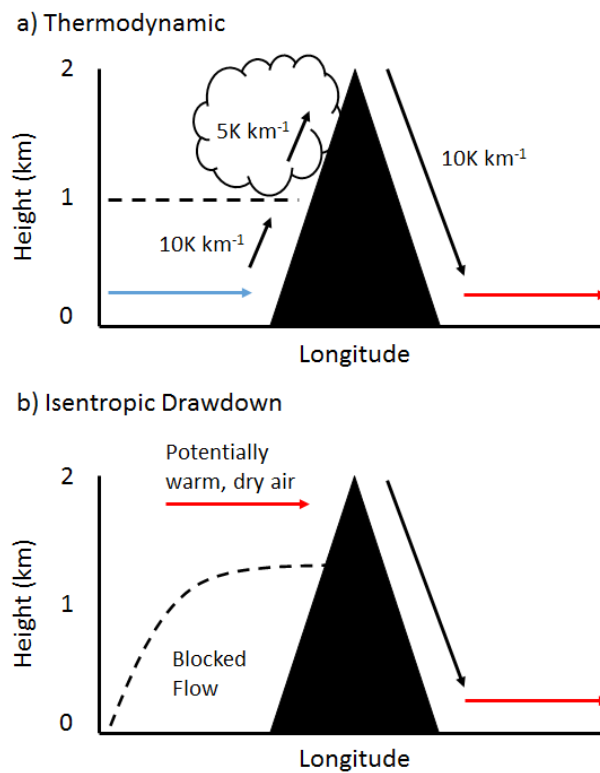
Figure 2: The thermodynamic (a) and isentropic drawdown (b) mechanisms responsible for föhn development over idealised topography.
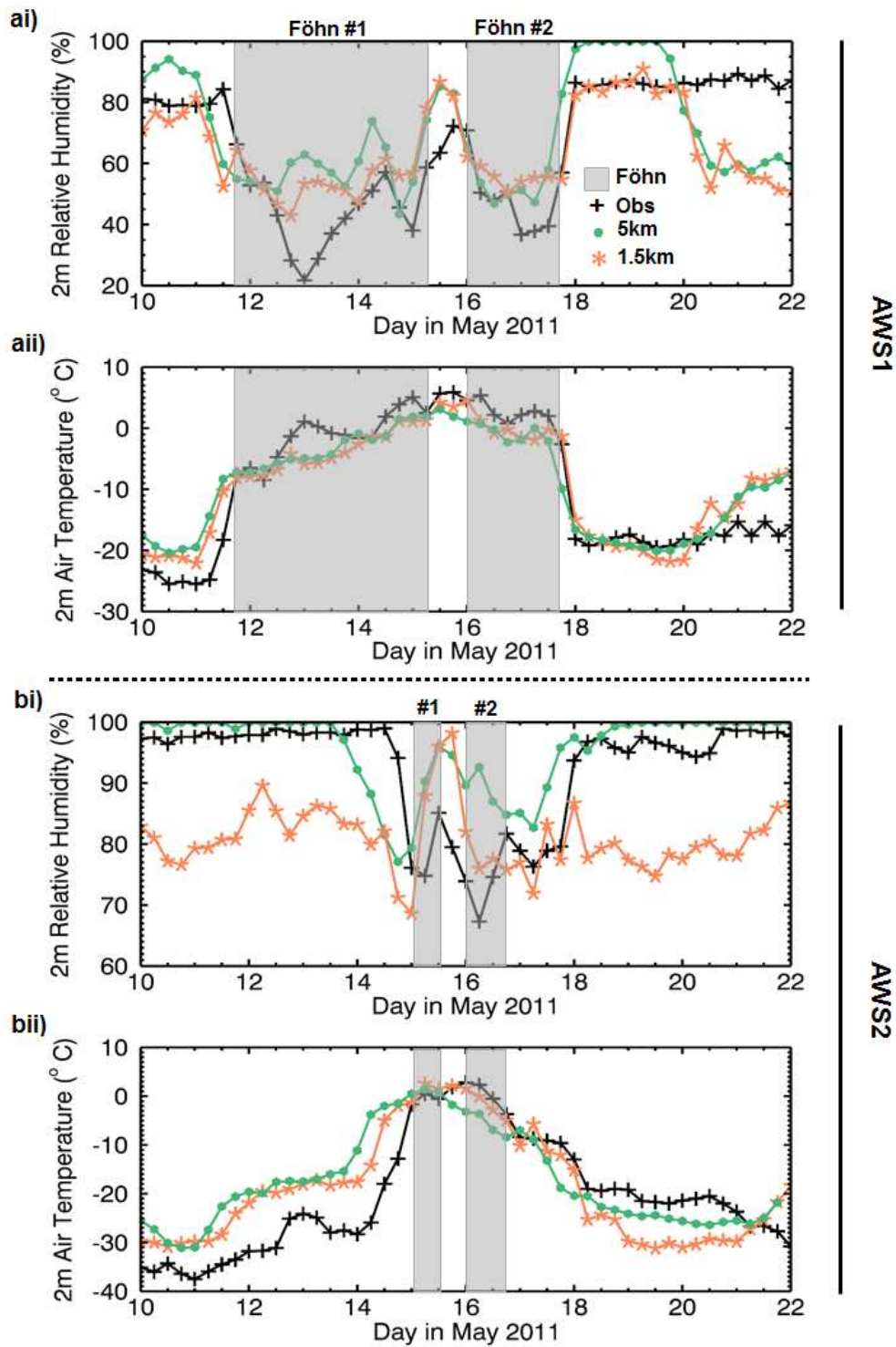
Figure 3: ai) The relative humidity and aii) air temperature at AWS1 from the 10th to 22nd May 2011. bi) The relative humidity and bii) air temperature at AWS2 for the same period. The observations from the AWS are shown by black crosses. The '5km' output is shown as green dots, and that from the '1.5km' run as orange stars. The grey boxes indicate the periods when two föhn events occurred. Föhn #1 and föhn #2 are abbreviated to #1 and #2 for the AWS2 plots.
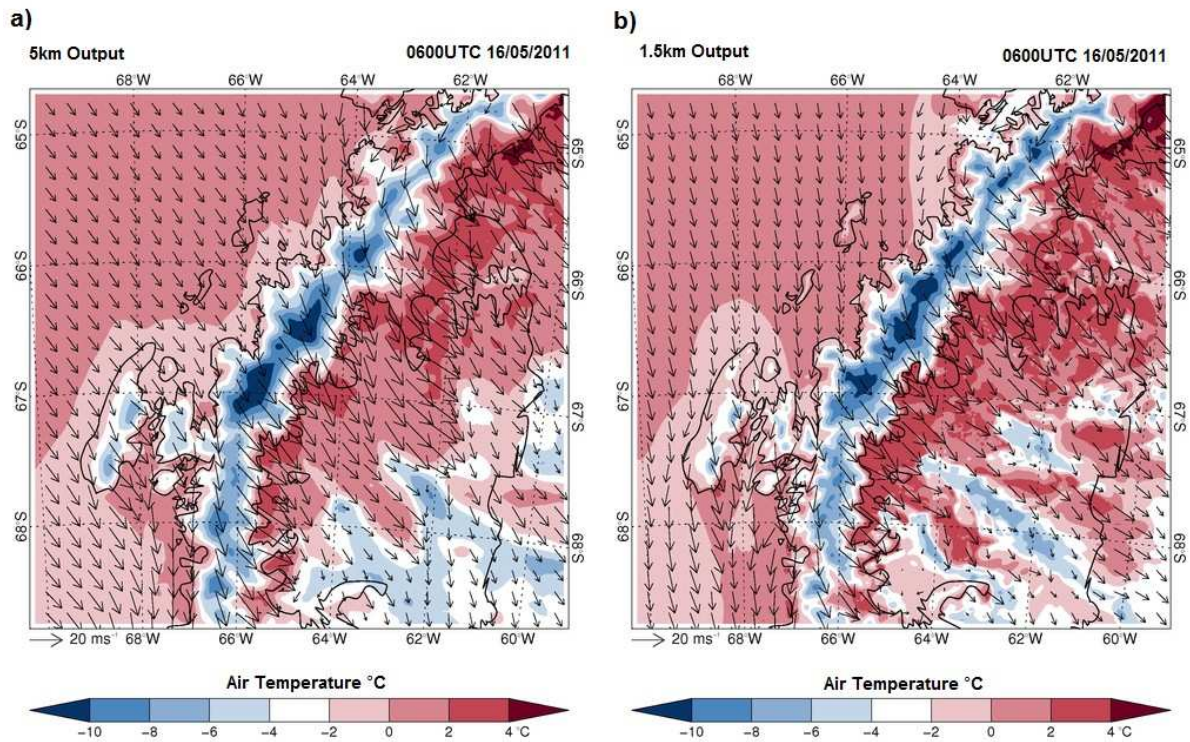
Figure 4: a) The 2m air temperature and 10m wind speed and direction simulated by the '5km' run and b) by the '1.5km' run. Output from both model runs is from 0600UTC on the 16th May 2011, six-hours after the start of the second föhn event at AWS1 and AWS2.
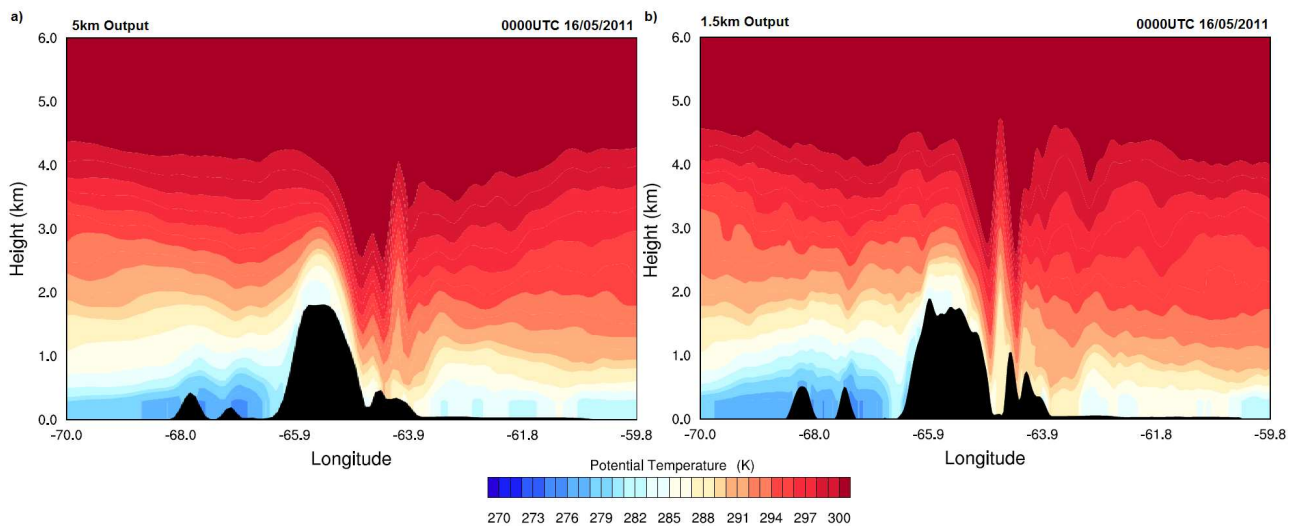
Figure 5: Cross section along 67°S of the Antarctic Peninsula of the simulated potential temperature (K) during föhn #2 from the '5km' run (a) and the '1.5km' run (b).

Table 1: The mean values, mean biases and correlation coefficient for air temperature, relative humidity and wind speed for the observations and both model runs from 10th-22nd May 2011. Green highlighted boxes are where the 1.5km resolution run was more accurate or the same as the 5km run. 'Obs' is the abbreviated version of observations.

		Mean			Mean Bias (Model-Obs)			Correlation		
	Data	T	RH	WS	T	RH	WS	T	RH	WS
AWS1	Obs	-10.7	66.9	4.0	-	-	-	-	-	-
	5km	-10.0	72.5	7.0	0.7	5.6	4.1	0.93	0.6	0.53
	1.5km	-10.2	65.6	7.4	0.5	-1.3	4.3	0.93	0.6	0.46
AWS2	Obs	-21.1	92.8	4.0	-	-	-	-	-	-
	5km	-18.0	98.6	5.1	3.1	5.8	1.1	0.84	0.3	0.74
	1.5km	-19.5	80.8	4.8	1.6	-12.1	0.8	0.82	0.08	0.84